Forest Science
https://doi.org/10.1007/s44391-026-00070-y

ORIGINAL ARTICLE

Drought on the Fly: UAS Mapping of Conifer Drought Stress

Lauren E. Lad[1] · Wade T. Tinkham[2] · Camille S. Stevens-Rumann[1] · Melanie Vanderhoof[3] · Jody Vogeler[4] · Alistair M. S. Smith[5]

Received: 13 May 2025 / Accepted: 12 May 2026

Abstract
Foliar moisture content (FMC) plays a crucial role in arid, frequent-fire forests by influencing fire behavior, tree survival, and serving as a proxy for tree health. Management actions such as mechanical thinning, flammable fuels reduction, and prescribed fires can act to mitigate wildfire risk and improve forest health by reducing fuel connectivity, diversifying forest structure, and creating canopy gaps. These management actions could be improved by the targeted removal of moisture stressed and potentially more flammable trees during treatments. However, maps of FMC are not widely available at the tree-level, with no existing products to map FMC of western conifers at the stand-level (< 0.25 m). This project focuses on the scalability of laboratory-developed models predicting sapling FMC to develop and assess tree-level FMC in natural forest conditions. Specifically, we tested whether existing FMC models accurately predict individual tree FMC using uncrewed aerial system (UAS) data. While laboratory-developed models did not translate well to field sites, a field-developed model achieved a mean absolute error of 6.5% FMC and 81% of predictions were within 10% FMC of the observed value. In ranking the observed and predicted FMC values, the field model successfully classified trees into FMC categories with up to 85.9% accuracy. This successful classification demonstrates the utility of UAS-based FMC mapping to inform management prescriptions. Integrating UAS-derived FMC monitoring into forest management could enhance forest resilience and adaptive capacity.

Keywords Foliar moisture content · Forest management · Uncrewed aerial system · Tree extraction · Machine learning

Introduction

Anthropogenic climate change is projected to increase the severity and intensity of drought across the southwestern United States (Cook et al. 2015), impacting conifer forests through compounding temperature increases and precipitation

Extended author information available on the last page of the article

Published online: 13 June 2026

deficits (Cook et al. 2018), resulting in decreasing soil water storage (Liu et al. 2019; Bolinger et al. 2023). Between 2000 and 2019 CE, southwestern North America experienced its second driest two decades since 800 CE, resulting in what has been described as a regional mega-drought (Williams et al. 2020). This region is projected to experience continued trends of increasing temperatures coupled with variable precipitation (Bolinger et al. 2023). Temperature-driven decreases in soil water availability and higher plant water demand contribute to plant-level physiological stress that reduces resilience to current and future drought (Breshears et al. 2005; Williams et al. 2022). Drought-induced resilience reductions in trees increase their susceptibility to fire and insect attacks (Sparks et al. 2024). Lower water availability affects trees by reducing foliar moisture content (FMC), nutrient uptake, and sap flux, all of which contribute to a tree's ability to withstand disturbances (Kreuzwieser and Gessler 2010; Ryan 2011). FMC and soil moisture content are also considered dominant drivers regulating the flammability of live and dead vegetation, respectively (Jolly and Johnson 2018; Schwilk et al. 2025). Drought stress is being compounded by stand density increases relative to historical norms (Mast et al. 1998) due to a legacy of fire suppression over the last century (Littell et al. 2016). Greater stand density increases forest water demands and further stresses trees (Zhang et al. 2019). These compounding climate and management-induced demands on moisture availability make forests increasingly susceptible to drought-, fire-, and insect-induced mortality (Williams et al. 2013).

A major indicator of water availability in forests is FMC, which responds to vegetation health and is a surrogate for individual plant resilience to weather, climatic oscillations, and disturbances (Keyes 2006; Zhang et al. 2019; Sparks et al. 2024). FMC changes daily based on evapotranspiration and water loss, or through precipitation and water uptake (Groover 2017). Beyond indicating the relative water content in plant material, FMC provides an estimate of fire risk and rate of spread (Jolly & Hadlow 2012).

The interaction of drought and stand density stressors contribute to elevated levels of tree mortality that can drive increases in fine, dead woody fuel accumulation (Ruthrof et al. 2016). Furthermore, the temperature driven decreases in surface fuel moisture elevate the likelihood of fire ignition, fire hazard, and extreme fire days (Alexander and Cruz 2013; Flannigan et al. 2016). Reduced moisture in both surface and canopy fuels increase the likelihood of fires transitioning from surface and ground fires into ladder fuels and the overstory, resulting in crown fires. Alterations to the drought, fire, and pest disturbance regimes, when coupled with persistent drought in an era of climate change, may facilitate changes to forest successional pathways that result in ecosystem conversion following disturbance-induced mortality (Batllori et al. 2020; Coop et al. 2020). Thus, considerations of current climate and projected climatic changes could help forest managers make informed decisions that reduce the likelihood of system conversion and maintain forest resilience to disturbances.

Conventional measures of foliar moisture require the collection of foliage from each plant and a comparison of the foliage's dry and wet (fresh) weight (Jolly and Hadlow 2012), providing a sample of data to represent an entire population. Similarly, leaf hyperspectral measurements can be used to estimate foliar moisture content of individual conifers (Zhou et al. 2021; Zhang et al. 2016). However, the need to sample individual plants and/or oven-dry specimens limits data extent and delays the availability of foliar moisture observations after collection. As such, there is limited capacity to collect rapid, spatially continuous measures of foliar moisture, particularly across management scales (i.e., 10 s to 100 s hectares). Satellite-based remote sensing can supplement field data collection to provide landscape-scale assessments of ecosystem stress (Lentile et al. 2006). Landsat (30 m resolution) and Sentinel-2 (10–20 m resolution), for example, are multispectral satellites that are used to monitor vegetation condition (Humagain et al. 2017; Hogland et al. 2019; Phiri et al. 2020). Plant water status is commonly assessed using spectral indices like the Normalized Difference Vegetation Index (NDVI; Rouse 1974), Normalized Difference Water Index (NDWI; Gao 1996), or thermal imagery (Pierce et al. 1990). These datasets, despite having high spatial resolution (> 10 m), average spectral data across multiple species, vegetation strata, and substrates within a single pixel, smoothing plant and species level variation (Lentile et al. 2006). Thus, forest managers cannot easily leverage this moderate spatial resolution to inform management decisions about which trees to retain or cut during thinning operations.

Uncrewed Aerial Systems (UAS) offer a potential solution to these limitations as the temporal resolution can be controlled by users and the high spatial resolution imagery can be finer than 3 cm (Perez-Rodriguez et al. 2020). Recent advances in UAS tree-level mapping have successfully created near-census maps of tree locations, heights, and diameters at breast height (DBHs) in dry, more open canopy conifer forests (Swayze et al. 2021; Tinkham et al. 2022). As these techniques become refined, UAS estimates of basal area and tree density achieve precisions of 5% to 10% (Tinkham and Woolsey 2024) and spatial patterns match field collected data (Hanna et al. 2024). Additionally, several studies have attempted to use UAS multispectral and thermal imagery to estimate FMC or similar vegetation moisture and health metrics for agricultural and crop tree (i.e., cherry, olive, citrus, and chestnut trees) applications with varying success (Ezenne et al. 2019; Blanco et al. 2020; Garza et al. 2020; Grulke et al. 2020; Padua et al. 2020; Marques et al. 2023). In a northeastern United States forest, Fraser and Congalton (2021) were able to classify trees as healthy, disturbed through either disease or pests, and degraded with 71% accuracy. In a European mixed-conifer forest, Abdollahnejad and Panagiotidis (2020) used multispectral imagery and a support vector machine classifier to classify leaf discoloration as an indicator of health with 84.7% accuracy. These studies show promise for tree-health assessments from UAS multispectral remote sensing, but no studies have examined the disturbance-adapted mixed-conifer forests of the Rocky Mountains, which are especially at risk for future drought events.

Previous work on individual conifer tree FMC remote sensing used a laboratory setting to develop a model to predict continuous FMC from the spectral bands available on a consumer-grade multispectral UAS camera for both a short-needle and long-needle conifer species (Lad et al. 2023). This effort used a spectroradiometer in a temperature and humidity-controlled laboratory to examine western white pine (*Pinus monticola* Douglas ex D. Don) and Douglas-fir (*Pseudotsuga menziesii* (Mirb.) Franco) at various levels of drought stress to classify drought status and predict FMC (Lad et al. 2023). Similar to studies monitoring crop FMC, Lad et al. (2023) found that indices such as the NDVI and PRI (Photochemical Reflectance Index), along with the red edge spectral range (700–720 nm) were the strongest predictors in modeling drought-stress in both short- and long-needle western conifers. Previous studies have also found PRI to be sensitive to real-time changes in photochemical efficiency (D'Odorico et al. 2021; Vicca et al. 2016), highlighting its utility for assessing tree health changes. Further, Sparks et al. (2016) found that a pre- and post-burning differenced NDVI quantified vegetation stress and burn severity with a high correlation to photosynthetic activity ($r^2 = 0.73–0.85$) following a laboratory burn. These modeling approaches, while promising, need to be validated through testing in mature forests of varying densities and drought conditions. Specifically, scaling these models to mature trees may present challenges to accurate quantification of FMC resulting from intra-tree variability or shadowing of lower branches.

Drought events, which decrease FMC, are and will continue to be a driving force of forest health and disturbance risk and recovery, underscoring its importance as a metric to describe forest conditions and to inform management actions. Although no comprehensive methods have yet been validated to predict tree-level FMC in forests, a preliminary assessment by Lad et al. (2023) found that a logistic regression and multiple linear regression model using NDVI, PRI, and red edge spectra were effective in identifying drought stress of saplings in a laboratory setting. Thus, the objectives of this study are to build off this prior work to test these laboratory-based models and compare their performance with field-based models in two mature mixed-conifer forests in northern Colorado. Using the laboratory developed model by Lad et al. (2023) we asked: Can laboratory-developed models of drought stress be used to identify the gradient of drought stress in mixed-conifer forests or are field-developed models necessary?

Methods

Study Area and Field Data Collection

To capture a gradient of FMC, this study was conducted at field sites with varying management histories and topographic complexities. The Red Feather Lakes (RFL) site is an untreated 6.0 hectare area of open mixed-conifer forest of ponderosa pine (*Pinus ponderosa* Lawson & C. Lawson) and Douglas-fir occupying a hill (slope = 1–45%) with all aspects represented and featuring exposed rocky outcroppings (Fig. 1). The Estes Park (EP) site is dominated by a northwesterly aspect on a 7–40% slope covering 4.2 hectares and was hand thinned in 2012 to create an open mixed-conifer stand of ponderosa pine and Douglas-fir. At both sites, a small number of Engelmann spruce (*Picea engelmannii* Parry ex Engelm.) and limber pine (*Pinus flexilis* E. James) are present.

We calculated mean annual temperature (T, °C) and mean annual precipitation (P, mm) using mean monthly values from PRISM (Parameter elevation Regression on Independent Slopes Model) 30-year normals (1991–2020) at 800 m resolution. These annual means allowed us to characterize typical climatic site conditions. At RFL and EP, mean annual temperatures were 5.6 °C and 7.9 °C while mean annual

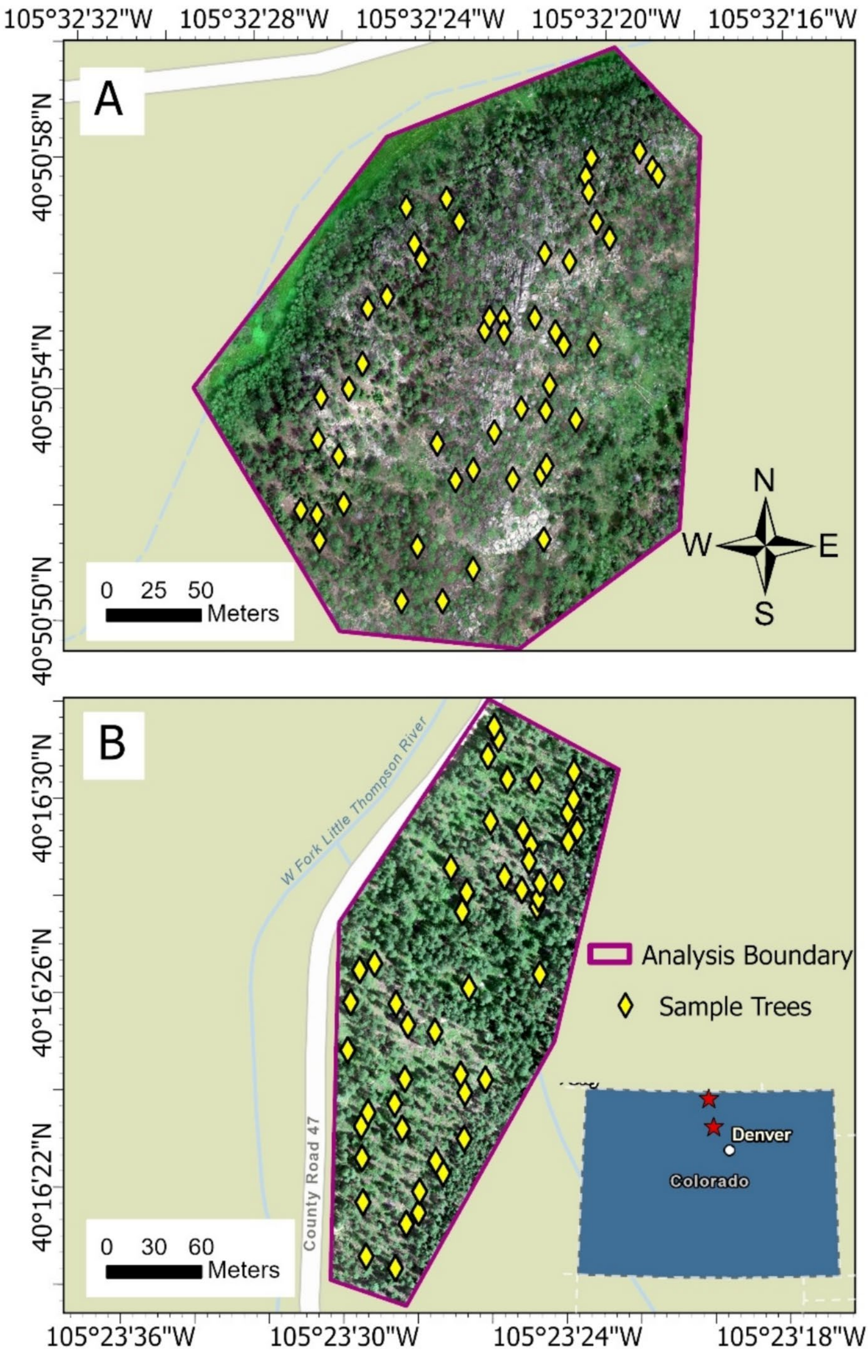

Fig. 1 UAS flight boundaries and derived true color imagery of the **A**) Red Feather Lakes (RFL) site and **B**) Estes Park (EP) site with the ESRI Outdoor base map. The northern star on the inset map is the Red Feather Lakes site and the southern star is the Estes Park site

precipitation was 444.7 mm and 525.1 mm, respectively. The precipitation received during the sampling year, 2023, was 503.7 mm at RFL and 564.3 mm at EP.

Prior to FMC monitoring, field survey trees were selected by randomly generating 50 points at each site, with the nearest dominant or codominant ponderosa pine or Douglas-fir tree identified for sampling. Limiting the survey to dominant and codominant trees was done to ensure reliable extraction from the UAS point cloud to allow for drought model testing. The sample trees had their height, DBH, crown base height (CBH), and species recorded, along with their location using an Emlid Reach RS2 + real-time kinematic GPS (Emlid Tech Kft, Budapest, Hungary).

Each site was sampled two times, for a total of four collection dates (July 25, July 27, September 18, and October 16) and 199 tree foliar moisture samples (Table 1). On each collection date, needle collection began at approximately 10:00 am and continued until 12:00 pm when UAS flights were conducted (Fig. 2). Following UAS flights, any remaining trees were sampled, with all moisture samples collected within 2 h of the UAS acquisition. Needle collection for each tree involved using loppers on an extending pole to clip bundles of needles in each cardinal direction and at varying heights. A minimum of four bundles were clipped from each tree and placed in a weighed and labeled plastic bag and stored in a cooler until they could be processed in the laboratory that afternoon. Variations in tree height and CBH meant that some samples could only be collected from the lower and middle third of the crown of some individuals. Testing was done on a subsample ($n=50$) of trees where FMC could be assessed in the lower, middle, and upper third of individual crowns, with a paired t-test showing no significant differences between FMC at different heights ($p=0.12$). Antecedent rainfall in the 48 h prior to collection was calculated from PRISM data as 0.33 and 0.00 mm at RFL for the first and second collection, respectively, and 0.73 and 1.16 mm at EP for the first and second collection, respectively (Table 1).

In the lab, bundles were removed from their plastic bag, needles and cones were stripped from the branch, and only the needles were added back to the bag. The fresh needle weight for each tree was measured by subtracting the weight of the plastic bag from the weight of the needles in the bag. All fresh weights were recorded within six hours of field sample collection. Then, needles were transferred to paper bags and dried in an oven at 105 degrees Celsius for at least 48 h, or until the dry weight had stabilized (Matthews 2010). Sample drying is optimized at this temperature due to the reduced relative humidity relative of ovens at lower temperatures (Matthews 2010). Once dry, the dry weight of each sample was measured by weighing the dried needles on a tared scale. All weights were recorded using an OHAUS scale with a precision of 0.01 g (OHAUS Corporation, Parsippany, NJ, USA). The FMC of each sample was calculated using Eq. 1 (Jolly and Hadlow 2012).

$$FoliarMoistureContent = \frac{(FreshWeight - DryWeight)}{DryWeight} x100 \tag{1}$$

UAS flights were conducted as close to 12:00 pm as possible to align with the sun's peak and reduce shadowing in the imagery. Acquisitions were conducted using a DJI Matrice 210 V2 (DJI, Shenzhen, China) with a Micasense RedEdge-MX

Table 1 Mean (standard deviation) of sample trees across the two study sites

Site	Ponderosa pine			Douglas-fir			First Collection			Second Collection		
	DBH (cm)	Height (m)	CBH (m)	DBH (cm)	Height (m)	CBH (m)	Julian Date	Temp (°C)	AR_{48} (mm)	Julian Date	Temp (°C)	AR_{48} (mm)
Estes Park (EP)	29.4 (7.7)	13.9 (2.2)	3.5 (1.0)	30.7 (12.4)	14.4 (3.5)	2.0 (1.0)	153	21.8	0.7	206	15.2	1.2
Red Feather Lakes (RFL)	29.0 (11.3)	10.2 (3.1)	2.4 (1.2)	22.3 (6.8)	9.3 (2.9)	0.7 (0.5)	151	21.9	0.3	234	17.1	0.0

Additionally, the Julian date, mean temperature and 48-h antecedent rainfall are given for each FMC collection. DBH: diameter at breast height, CBH: canopy base height, AR_{48}: 48-h antecedent rainfall

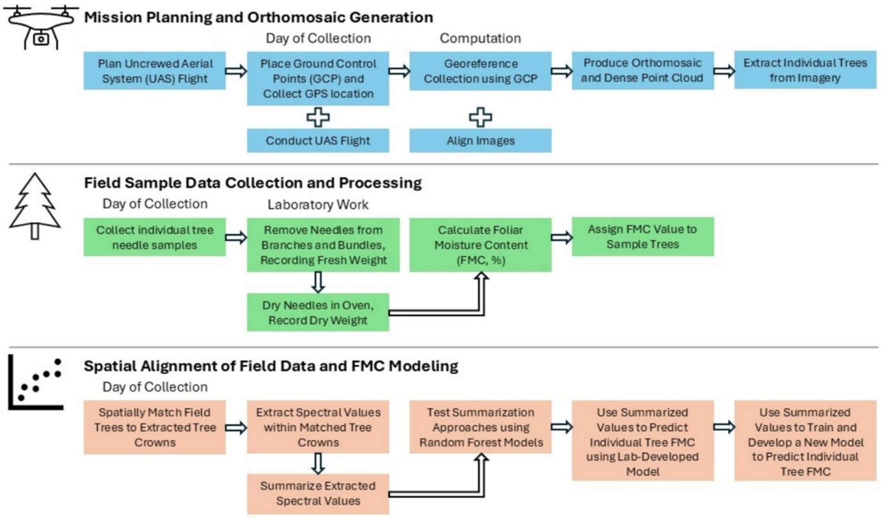

Fig. 2 Workflow diagram outlining (top) Uncrewed Aerial System (UAS) collection and processing, (middle) field tree foliar moisture content (FMC) processing, and (bottom) data alignment and modeling of FMC

10-band Dual-Camera system attached (AgEagle Aerial Systems Inc., Wichita, KS, USA) and lasted an average of 20 min at each site. All flights used a serpentine flight pattern at 90 m above ground level and at a speed of 6 m s^{-1} with 85% forward and 80% cross-track image overlap and nadir viewing angle. The Micasense system captured 10-band multispectral imagery (Supplemental A) at 6.3 cm resolution. Prior to takeoff and immediately after landing, manual captures were taken of the Micasense reflectance panels in full sunlight. These images allowed us to capture ~ 50% reflectance and were used to correct inconsistencies in lighting during the flights. Ten ground control points (GCPs) were used at each site to ensure spatial alignment of the imagery with the field recorded tree locations. The GCPs were chosen based on visibility from above, spacing across the sites, and had their locations recorded using an Emlid Reach RS2 + real-time kinematic GPS. The GCPs had a reported average horizontal and vertical root mean square error of 0.038 m and 0.077 m, respectively.

UAS Image Processing

For each of the four acquisitions, UAS images were processed in Agisoft Metashape version 1.6.4 (Agisoft LLC., St. Petersburg, Russia) using the Structure from Motion algorithm with Mild Depth Map Filtering and High-Quality generation parameters. These settings were used to maximize individual tree extraction accuracy based on the findings of Tinkham and Swayze (2021). The sun sensor and photos of the reflectance panels were used to calibrate image spectral reflectance and correct for lighting inconsistencies due to clouds and sun angle.

The GCP locations were imported to Metashape and iteratively georeferenced using a minimum of 10 photos per GCP, resulting in a median (standard deviation) root mean square error of 7.3 (5.2) cm, 5.8 (3.5) cm, and 0.8 (0.5) cm for X, Y, and Z locations, respectively across the four collections. Once GCPs were georeferenced, UAS photos were aligned to produce approximately 5–8 million tie points as well as an orthomosaic and dense point cloud with information for the 10 spectral bands attached. No tie points were removed for error reduction. The orthomosaics had a final pixel resolution of 6.3 cm. Then, orthomosaics and point clouds were exported as GeoTIFFs and LAS files, respectively, for each flight date in the North American Datum 1983 UTM Zone 13 North (NAD83, UTM 13 N) projected coordinate system with ellipsoidal heights referenced to the Geodetic Reference System 1980 (GRS80) ellipsoid. For each collection, values for each spectral band were normalized to the reflectance scale by dividing each cell value for a given band by the global maximum for that band (Micasense).

UAS Tree Extraction

To extract individual trees and tree crowns, point clouds and orthomosaics were processed in RStudio version 4.3.2 (R Core Team 2023). Following the point cloud processing steps from Tinkham and Woolsey (2024), point clouds were processed using the cloud2trees package (Woolsey 2024) which integrates the lasR (Roussel 2024) and lidR packages (Roussel et al. 2020; Roussel and Auty 2024). First, raw point clouds were denoised which involved identifying isolated points and removing them, as well as duplicate points, from the point cloud. Then, we classified ground points and generated a digital terrain model (DTM) with 1.0 m resolution using Delaunay triangulation and pit filling. Pit filling was used to correct artificial depressions in the DTM that result from interpolation artifacts or misclassified points in areas with rocky outcroppings, ensuring a realistic and continuous ground surface. The ground-classified points were used to create a triangulated surface to height normalize the point cloud and generate a canopy height model (CHM) at 0.10 m resolution. To locate individual trees, we used a variable window function [Eq. 2] as proposed by Creasy et al. (2021) and the “locate_trees” function from the lidR package to identify all tree tops that were at least 2 m tall.

$$VariableWindowRadius = 0.3 + CHMValue * 0.1 \tag{2}$$

Then, we delineated tree crowns using the marker-controlled watershed function of the ForestTools package. Finally, we spatially joined the tree tops with the tree crowns following the methods of Tinkham et al. (2022). The outputs of these steps included a CHM and DTM raster, individual tree crown polygons, and tree location points which included the extracted height.

The tree location points were spatially matched to field-collected tree locations following the methods of Tinkham et al. (2022) for ponderosa pine. This spatial matching process used a maximum search distance of 5 m and a maximum height error of 4 m to identify the nearest UAS trees to a field tree using the sf package (Pebesma 2018). The UAS tree within the search distance with the smallest height error was then assigned to the field tree as a match. This process iterated over each field tree until all

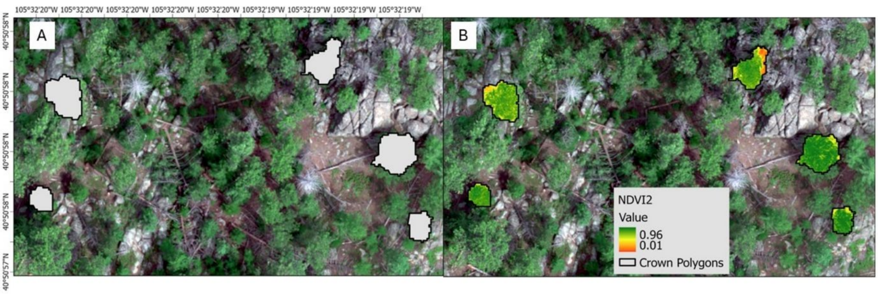

Fig. 3 Random subset of extracted tree polygons showing **A**) true color imagery and **B**) their calculated Normalized Difference Vegetation Index 2 (NDVI2) value on top of UAS-derived true color imagery of the Red Feather Lakes (RFL) site. The within tree crown polygons pixels were used to calculate mean, median, and every 10th-90th percentile values as potential predictors of tree foliar moisture content. The true color image and derived NDVI2 are from the RFL site on July 25, 2022

field trees were matched with an UAS extracted tree. These matches were used with the "st_intersects" function from the sf package to extract the corresponding individual tree crown polygon. Then, using the individual tree crown polygons and 10-band orthomosaics, we derived each pixel's spectral values for each of the 10 bands within each crown polygon using the "exact_extract" function of the exactextractr package (Baston 2020); Fig. 3). Using the extracted normalized cell values for each tree, we calculated NDVI2 (Eq. 3), PRI (Eq. 4), and Foliar Moisture Content Indicator (FMCI, Eq. 5). Raster values within each tree crown polygon were further summarized as the mean, median, 10th, 20th, 25th, 30th, 40th, 60th, 70th, 75th, 80th, and 90th percentile band and index values. The summarized raster values were then tested as predictor variables in the multiple linear regression model developed by Lad et al. (2023). We also evaluated species as a potential predictor variable.

$$NDVI2 = \frac{NIR - Red2}{NIR + Red2} \tag{3}$$

$$PRI = \frac{Green2 - Green}{Green2 + Green} \tag{4}$$

$$FMCI = \frac{RedEdge3 - NIR}{RedEdge3 + NIR} \tag{5}$$

Modeling and Data Analysis

After summarizing predictor variables by tree crown, we tested the laboratory developed Multiple Linear Regression Model (MLRM; Eq. 6) from Lad et al. (2023) which used NDVI2, PRI, FMCI, and the RedEdge3 band as predictor variables of FMC.

$$FMC\% = -226.61 + 138.64 \times NDVI2 + 611.92 \times RedEdge3 + 851.31 \times FMCI + 1039.63 \times PRI \tag{6}$$

We used the stats package in base R (R Core Team 2023) and tested the Lad et al. (2023) model using each of the 12 crown summarization techniques (i.e., mean, median, 10, 20, 25, 30, 40, 60, 70, 75, 80, 90 percentile) with the model's four variables (NDVI2, PRI, FMCI, RedEdge3). These summarization approaches were tested to maximize accuracy when scaling from laboratory to field tree sizes. We compared the accuracy of the 12 versions of the MLRM in predicting observed FMC using Pearson's correlation, mean error (ME), and root mean square error (RMSE). Pearson's correlation was used to evaluate the strength of the linear relationship between predicted and observed FMC values, providing insight into how well the model captures overall variance in FMC. To assess systematic bias in model predictions, we performed a paired t-test comparing the mean observed FMC to the mean model-predicted FMC. Additionally, we examined the model's ability to rank trees by relative drought stress using Spearman's rank correlation. Unlike Pearson's correlation, which assumes a linear relationship, Spearman's correlation assesses monotonic relationships and is robust to non-linearity. This allowed us to determine how well the model preserves the relative ordering of trees based on their FMC values.

To identify potential differences between the laboratory model and the optimal prediction of FMC using field scale data, we also fit a series of new multiple linear regression models using the UAS-derived tree-level spectral bands and indices, along with species and Julian date to predict FMC. Variable selection for the field-based MLRM was performed by fitting Random Forest models using the RandomForest R package (Breiman 2001; Liaw and Wiener 2002). Random Forest uses an ensemble learning approach, constructing multiple decision trees and aggregates their results to improve prediction accuracy and reduce overfitting. This approach was chosen for its ability to handle high-dimensional predictor sets and accommodate potential relationships. Models were fit to each of the 12 sets of crown summarization metrics (e.g., 10th, 20th, 30th percentile, etc.) to identify the set of metrics best suited to predict FMC with ntrees = 199, specifying the number of decision trees, and mtry = 6, the number of variables randomly sampled at each split. The models included the tree-level summary metrics for the ten spectral bands and nine spectral indices (19 variables). These spectral indices included NDVI, NDVI2, PRI, FMCI, NDWI (Eq. 7), Green Normalized Difference Vegetation Index (GNDVI; Eq. 8), and Normalized Difference Red Edge (NDRE; Eq. 9). The best Random Forest regression model was identified as the model with the greatest variance explained (R^2).

$$NDWI = \frac{Green - NIR}{Green + NIR} \tag{7}$$

$$GNDVI = \frac{NIR - Green}{NIR + Green} \tag{8}$$

$$NDRE = \frac{NIR - RedEdge1}{NIR + RedEdge1} \tag{9}$$

For the crown summarization techniques with the highest performing Random Forest model, we tested variable correlation to remove any highly (i.e., > 70%) collinear variables. When two variables were highly correlated, we retained the variable more strongly related to FMC. This reduced set of non-collinear predictors was then used to construct a multiple linear regression model in R using the stats package (R Core Team 2023). The model was reduced using a forward–backward stepwise approach to minimize the Akaike Information Criterion (AIC) using the olsrr R package (Hebbali 2020). This approach identified the most parsimonious model while retaining key predictors of FMC. To avoid overfitting, model development and evaluation were conducted using a 70/30 training and testing split, and predictive stability was assessed using fivefold cross-validation. To quantify uncertainty and assess model consistency, we estimated predictor coefficients and their 95% confidence intervals using bootstrapping with 1,000 repetitions (boot package; Davison and Hinkley 1997; Canty and Ripley 2022). To evaluate the practical utility of the final model, we ranked the model-predicted and field-observed FMC values from lowest to highest and categorized trees into two groups based on their rank percentiles. Specifically, we assessed the model's ability to correctly distinguish the most drought-stressed subset of trees by dividing the dataset at thresholds of 10%, 20%, 30%, 40%, and 50% of the lowest FMC values. This analysis was designed to simulate how a forest manager might use the model to prioritize trees for targeted intervention, ensuring that the method effectively identifies the most drought-stressed individuals.

Results

Sample Structure

Field collected FMC was approximately normally distributed when examined across all sites and dates (Fig. 4). The observed FMC values ranged from 73 to 126%, with an average of 98.4%. FMC across the four dates was bimodally distributed, but the range of FMC values tended to narrow through time. Additionally, the FMC values at EP were, on average, higher than at RFL, where rainfall is lower, and FMC values were generally higher for Douglas-fir compared to ponderosa pine (Fig. 4).

Spectral reflectance of bands and indices were also compared across Julian dates to examine the importance of the collection date (Fig. 5). Most spectral bands exhibited low variation between Julian dates, except for the first data collection which consistently had greater reflectance levels. Within a single collection date, bands in the red and red edge portion of the spectrum featured greater variability and wider interquartile ranges than bands with shorter wavelengths. The near-infrared indices (NDVI2 and FMCI) exhibited lower mean values for the RFL collections (first and last Julian date) compared to the EP collections, with there being much more consistency in the PRI values between dates, but less within site variation.

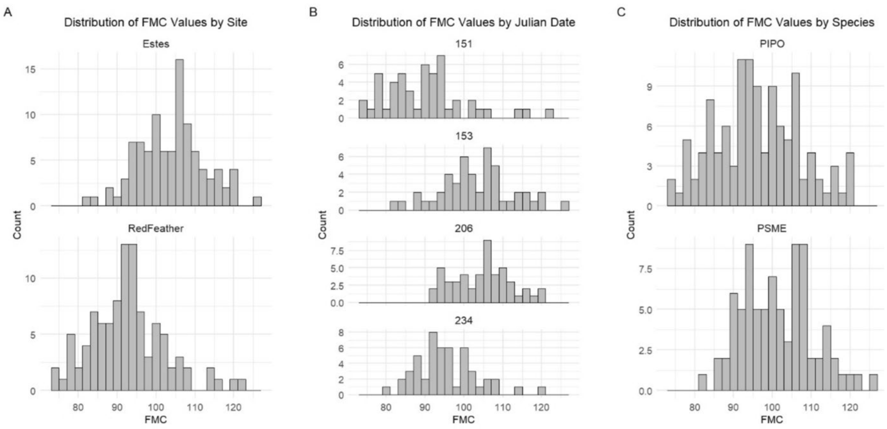

Fig. 4 Histograms of foliar moisture content values across the four collections at the Red Feather Lakes (RFL) and Estes Park (EP) sites separated into **A**) distribution by site, **B**) distribution by Julian date, and **C**) distribution by species. PIPO: ponderosa pine; PSME: Douglas-fir

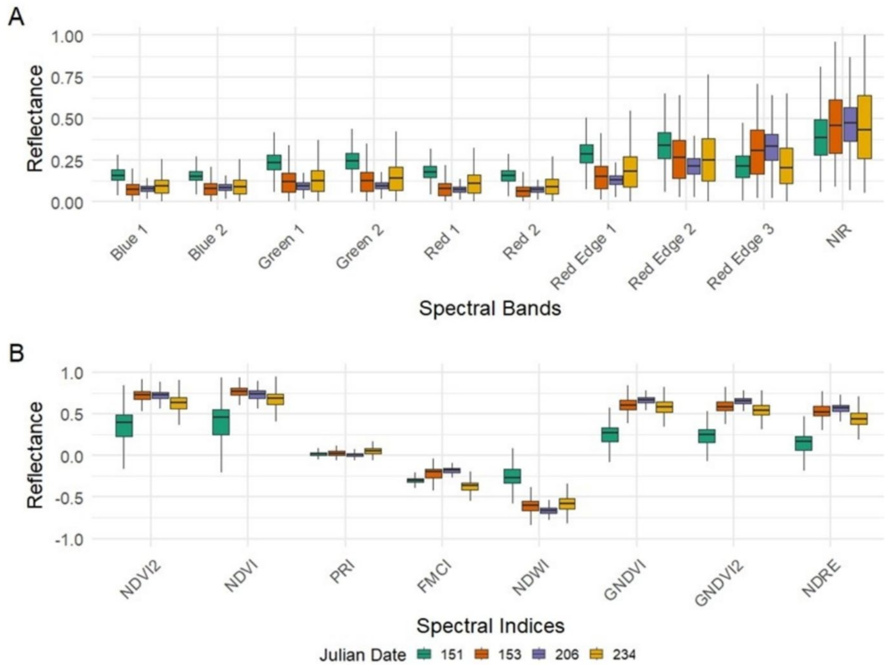

Fig. 5 Boxplot of **A**) spectral band and **B**) index distribution within surveyed tree crowns colored by Julian Date. NIR: near infrared; NDVI: Normalized Differenced Vegetation Index; PRI: Photochemical reflectance index; FMCI: Foliar Moisture Content Index; GNDVI: green NDVI; NDRE: Normalized Differenced Red Edge

Existing Laboratory Model Performance

Comparing the MLRM predictions from the 12 crown summarization techniques, using the Lad et al. (2023) equation, a paired t-test of the observed and predicted values found significant differences between means using the 90th percentile ($p=0.01$) and mean ($p=0.03$) techniques. Across the 12 summarized models, the observed versus predicted correlation peaked using the mean summarization technique. We observed lower correlation values with both lower percentile and higher percentile summarization techniques of within canopy values (Table 2). Conversely, the ME and RMSE decreased with the use of higher percentiles, suggesting an increase in accuracy of the predicted values. However, the ME and RMSE suggest that predictions from all 12 models were relatively imprecise. Testing the ranking of the predicted FMC values from the mean and 90th percentile models against the observed rankings using the Spearman's rank correlation showed that both models performed similarly (Fig. 6).

Field Model Performance

The random forest models identified that using the 10th percentile of pixel spectral values within a tree crown explained the most variation (variance explained = 26.62%) in tree-level FMC with the smallest mean squared error (MSE = 86.46; Supplemental B). In our testing of summarization approaches, species was a significant predictor of FMC in ten out of twelve of the random forest models, highlighting its utility (Supplemental C). The final reduced multiple linear regression model developed on the field data retained species and the within crown

Table 2 Accuracy of each within crown summarization metric tested in applying the multiple linear regression model from Lad et al. (2023)

Summarization Metric	Pearson's Correlation	Mean Error	Root Mean Square Error	p-value
Mean	0.437	203.77	238.44	<0.05
Median	0.414	197.08	237.00	<0.05
10th Percentile	0.421	411.86	431.77	<0.05
20th Percentile	0.422	345.18	368.12	<0.05
25th Percentile	0.423	317.33	342.09	<0.05
30th Percentile	0.421	291.50	318.50	<0.05
40th Percentile	0.417	242.94	275.42	<0.05
60th Percentile	0.412	153.16	202.91	<0.05
70th Percentile	0.409	109.54	173.04	<0.05
75th Percentile	0.408	86.89	159.92	<0.05
80th Percentile	0.405	63.14	148.40	<0.05
90th Percentile	0.398	55.53	135.66	<0.05

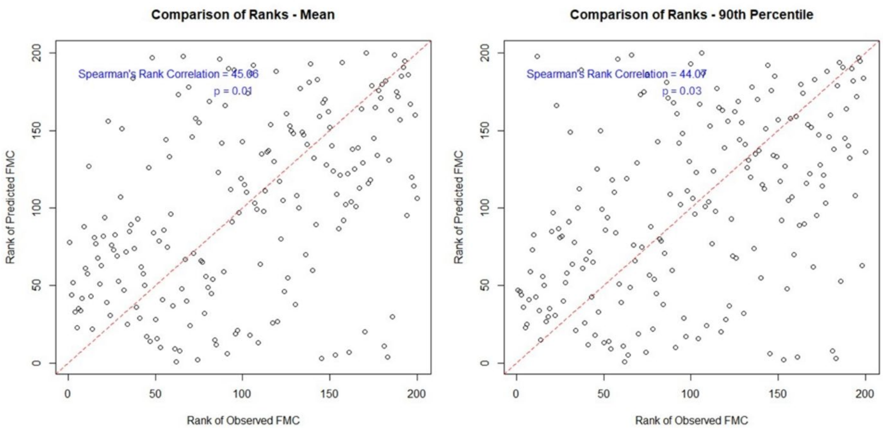

Fig. 6 Observed versus predicted foliar moisture content (FMC) ranks from the two highest performing multiple linear regression models, based on Lad et al. (2023), using (left) the mean spectral values per crown, and (right) the 90th percentile spectral values per crown

Table 3 Multiple linear regression model output table using the 10th percentile of summarized tree crown spectral data

	Coefficient	95% Confidence Interval	Standard Error	t value	p-value
Intercept	94.376	89.16—99.85	2.804	33.654	< 0.0001
Douglas-fir	11.270	6.19—16.23	2.255	4.997	< 0.0001
NDRE	31.421	22.75—40.00	3.858	8.145	< 0.0001
FMCI	22.175	10.99—32.72	6.460	3.433	0.0007
Douglas-fir:NDRE	−21.839	−35.48—−8.90	5.903	−3.699	0.0003

10th percentile values of NDRE and FMCI as predictors (Table 3), resulting in an adjusted R^2 of 0.373 ($p < 0.0001$) with a residual standard error of 8.45% FMC. Predicted FMC increased as the index score increased for both NDVI2 and FMCI (Fig. 7). However, species was significant with Douglas-fir increasing the intercept by 11.3% FMC and decreasing the NRDE coefficient by about two-thirds compared to the ponderosa pine predictions.

Evaluation of the observed and predicted FMC values shows that the multiple linear regression model captured the general trend in FMC values and provides an unbiased representation of the relationship (Fig. 8). Dissecting the predictions showed that 46% were within 5% of the observed FMC value, with 81% within 10% of the observed FMC value. Evaluation of the model residuals shows that the EP site had a slight negative FMC prediction bias (−0.384), while RFL had a slight positive prediction bias (0.380). Additionally, prediction biases transitioned from −1.10 for the earliest Julian date to being 0.59 for the last Julian date.

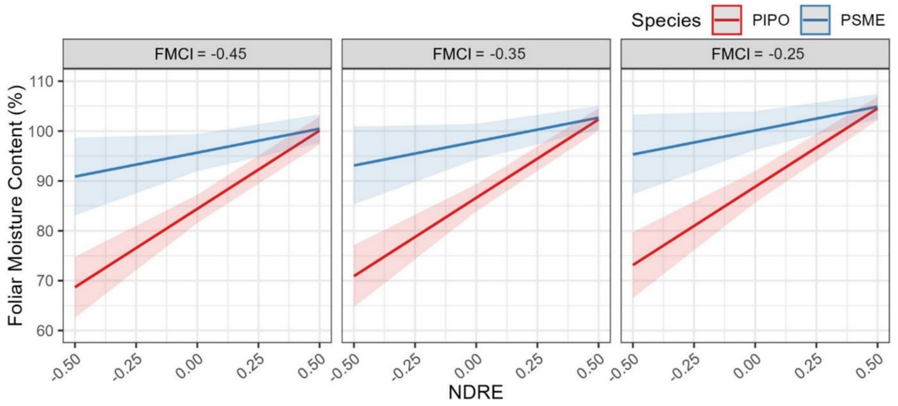

Fig. 7 Predicted effects of the 10th percentile values of NDRE and FMCI in a multiple linear regression model separated by species. Shaded areas indicate 95% confidence intervals for predictions. PIPO: ponderosa pine; PSME: Douglas-fir; NDRE: Normalized Differenced Red Edge; FMCI: foliar moisture content index

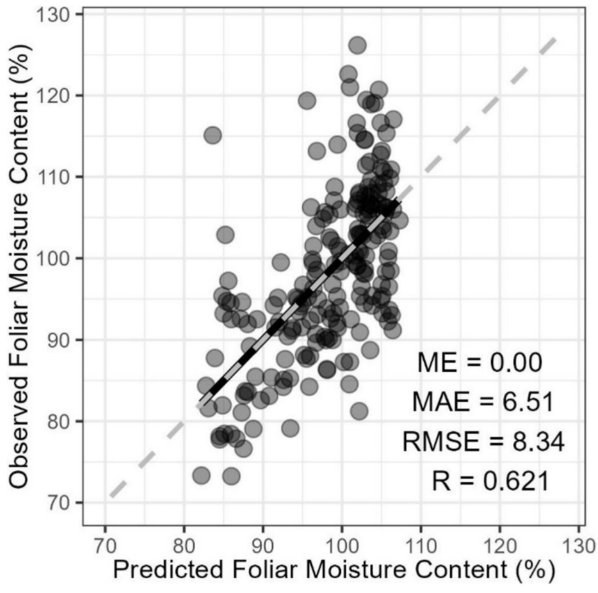

Fig. 8 Observed and predicted foliar moisture content from a multiple linear regression model using species and the 10th percentile values of NDRE and FMCI as predictor variables. ME: mean error; MAE: mean absolute error; RMSE: root mean squared error; R: Pearson's correlation coefficient

Comparing the ranking of the observed and predicted values as binary classes of the lowest 50% of FMC and highest 50% of FMC achieved a classification accuracy of 60.8% ($p = 0.002$). Repeating this process to include splits identifying the 10%, 20%, 30%, 40%, and 50% most drought stressed trees resulted in an average accuracy of 70.5%, with accuracy declining from 85.9% for the 10/90 split to 60.8% for the 50/50 split. However, predicted bins were only statistically significant (i.e., $p < 0.05$) when identifying the 50% most drought stressed trees.

Discussion

Model Outcomes

When UAS derived values were applied to the prediction of FMC, the laboratory developed MLRM achieved relatively low prediction accuracy, relative to the field-based model ($R = 0.437$ compared to $R = 0.62$, respectively), suggesting the field-based model better capture the relative gradient of tree FMC. However, the field-based multiple linear regression model fit using the UAS data predicted FMC with a mean absolute error of ~ 6.5%. Simultaneously, the mean absolute errors varied between 7.6% and 5.2% FMC from the earliest to most recent Julian dates, which is unsurprising as FMC can change rapidly in the field with greater fluctuations earlier in the growing season and diurnal variability of FMC at its narrowest in late summer for western US conifers (Philpot 1965). Matús et al. (2025) also found seasonal moisture stress was most distinct in late summer and autumn. Additionally, the movement of carbohydrates within plant tissue seasonally can also influence how the same amount of moisture converts to FMC (Larcher 2003). These temporal fluctuations mean that a prediction of FMC at a single time point may not necessarily represent the health of an individual tree. However, mid-day acquisitions minimize within-tree relative FMC (Philpot 1965), while reducing shadowing in imagery. FMC for Douglas-fir and ponderosa pine has been documented as between 100 and 130% in the summer with old foliage having values commonly under 100% (Keyes 2006). Interestingly, our field observed average FMC across summer collection dates was 98%, with many trees below 90% FMC. The EP site had consistently higher FMC values, potentially a consequence of this site being in a post-treatment condition, while the RFL site has higher forest density and has not been treated or disturbed in the last 100 years. However, work in other ponderosa pine forests has not found an effect of treatment on foliar moisture content (Faiella and Bailey 2007). Variation in prediction bias with both site and Julian date suggests that environmental covariates may play an important role in improving model fit, as abiotic factors such as topography and hydrology influence tree physiology (Ewane et al. 2023).

The field developed MLRM successfully classified trees into higher versus lower drought-stress categories with 70.5% accuracy. Our success in classifying the most drought-stressed trees suggests that rank-based thresholding can maximize the accuracy of a decision-support tool for identifying the gradient of drought-stress. By converting continuous FMC predictions into binary classifications, we achieved relatively high mean classification accuracy (70.5%), with the highest accuracy (85.9%) occurring when identifying the most drought-stressed 10% of trees. However, accuracy declined as the classification included a larger proportion of the drought-stressed trees. This trend suggests that a rank-based classification approach could allow managers to effectively target trees most in need of intervention.

Our binary classification (stressed/not stressed) had lower accuracy than previous studies attempting to classify tree health status using UAS multispectral imagery in orchards (healthy/unhealthy 97.5%; Jemaa et al. 2023), but similar to the accuracy achieved by other efforts in mixed broadleaf-conifer forests (live/dead/

beetle infested 84.7%; Abdollahnejad and Panagiotidis 2020) and in early bark beetle detection (81% accuracy; Näsi et al. 2018). However, no studies to date have identified the relative health of western US mixed-conifer forests at the scale of individual trees. Previous efforts have connected hyperspectral and thermal imagery with field observations of stomatal conductance (Zarco-Tejada et al. 2013), while other assessments have used short-wave infrared data (1557–2082 nm) to classify drought-stress induced changes (Matús et al. 2025). As UAS sensor technology and efforts to integrate hyperspectral, short-wave infrared, or thermal imagery continue to advance, model accuracy of FMC and other health metrics will likely continue to improve.

The lack of high accuracy in the lab-developed MLRM (Lad et al. 2023) could be the result of scaling and summarization mismatches. In the lab, pure individual sapling spectral values were collected using three plant probe samples across the crown, while in the field, tree spectral values were collected as pixels across entire tree crowns, with values primarily reflecting the top 2D profile of the crown. We tested summarization techniques to account for the mixture of foliage, branch, and background substrate captured in the UAS pixels. However, the UAS imagery also contended with greater spectral variability in mature crowns as, even within extracted polygons, there are differences in crown shading/illumination. Consequently, the laboratory saplings (Supplemental C) had a reduced spectral distribution compared to the UAS imagery. Additionally, the young needles (i.e., less than two years old) on the laboratory saplings likely reflect more light (Rock et al. 1994) compared to the older (i.e., up to five years old) needles assessed in the field. The reduced spectral variability in the training data for the laboratory MLRM likely contributed to the relatively poor model prediction using the UAS spectral data, as the UAS spectra contained needles of varying age and status along with a mixture of background material. Overall, UAS monitoring shows strong potential for assessing individual tree moisture stress, but detectability of characteristics like FMC is variable. Since FMC is determined by a multitude of environmental and abiotic factors such as soil moisture, temperature and precipitation, topography, biomass, and stand density, future studies may benefit from incorporating these factors in their models (Park Williams et al. 2013; Faiella et al. 2007; Brown et al. 2022; Zhang et al. 2019). Additionally, future tree health assessments could benefit by designing sampling to consider site-level abiotic variability, in addition to using new sensors that include short-wave infrared and thermal spectra.

Management Implications

Forest FMC is an important indicator of forest resilience and the relative distribution of FMC within a site can highlight areas for targeted management actions. At our post-treatment site, Estes Park, mean FMC was 11% higher than at the untreated Red Feather Lakes site, consistent with previous studies that found a significant relationship between decreased stand density and increased moisture availability (Simonin et al. 2007; Andrews et al. 2020; Young et al. 2023). This increase in moisture availability also increases tree growth and decreases sensitivity to changes in climate (Finley and Zhang 2019). Thus, our models of site-specific relative FMC could be applied to forest sites and provide managers with relative tree stress metrics to inform targeted thinning and prescribed fire operations.

Informed management is important for maintaining and improving forest health, particularly as drought stress reduces tree productivity and carbon and nitrogen uptake (Joseph et al. 2021). Extreme drought can induce widespread mortality events, particularly if the drought is prolonged (Allen et al. 2010). Climate stress is already exceeding species' physiological drought tolerance, resulting in tree mortality within the drier parts of species' ranges (Anderegg et al. 2019a, b), thus better understanding tree stress when implementing treatments is critical. While the mortality of overstory trees can initially decrease crown fire potential it can also increase surface fire intensity (Stephens et al. 2018). Beyond fire dynamics, stand-level resilience to drought is also shaped by physiological and structural diversity. Plant hydraulic diversity has been shown to enhance forest resilience to drought (Anderegg et al. 2018), and maintaining size class diversity may mitigate drought impacts, as higher soil moisture availability can support understory plant water content and delay overstory canopy stress (Brown et al. 2022). As climate change and associated drought stress and fire risk continues to push the bounds of forest resilience, anticipating future climatic pressures and adjusting accordingly will be increasingly important.

Tree-level relative FMC, combined with tree size and spatial arrangement data, can guide thinning, prescribed fire, and restoration treatments to achieve increases in the vertical and horizontal complexity of forests, while prioritizing the retention of the site's most resilient individuals (Churchill et al. 2013). These actions have been shown to be most effective at reducing wildfire severity and effects when applied together (Davis et al. 2024). This study's FMC rankings could serve as a weighting factor to identify trees for removal or retention during thinning operations. By identifying areas with historically persistent openings, managers can potentially pinpoint locations where infilling trees are likely drought-stressed due to soil moisture and nutrient limitations (Bond and Keeley 2005) and prioritize thinning in those areas (Larson and Churchill 2012). Additionally, these models could be used to evaluate sites post-thinning to examine changes to moisture content of the remaining trees (North et al. 2009). Connecting our model of tree-level FMC with ecologically informed management, we can increase the information available for adaptive management that balances forest resilience and fire risk reduction. By comparing pre- and post-treatment FMC, it would be possible for managers to refine best practices for reducing competition, increasing drought resilience, and improving stand health.

In fire-dependent forests, prescribed fire is a useful management tool for reducing fuel availability and connectivity, potentially decreasing subsequent fire behavior (Prichard et al. 2020). Prescribed fire planning relies heavily on weather data which informs fuel conditions and predicted fire behavior (Ryan et al. 2013). Integrating models of FMC into this planning process could provide data on live fuel moisture, improving fire behavior predictions. Relative FMC can fluctuate with weather (Keyes 2006) and provides valuable information about fuel moisture levels and combustibility, which could guide ignition strategies, allowing managers to adjust ignition line distance to control fireline intensity based on burn-specific mortality objectives. Providing managers with near-real-time access to overstory fuel conditions could enhance data-driven fire planning decisions. Further, these models could also be applied to assess the resilience of surviving trees after initial fires and inform post-fire thinning and refugia management to increase resistance to subsequent drought and wildfire.

The effectiveness of UAS-derived models to infer FMC has considerable implications for the assessment of fire ignition risk due to the relative flammability of live vegetation. Specifically, the flammability of live vegetation within and adjacent to critical infrastructure such as power lines, schools, and airports is a key monitoring need that UAS data could be used to address. For example, flying UAS in remote tracts of land along the path of power lines could enable rapid and predictive monitoring of live fuel flammability, fuel type, and fuel abundance in the power line right-of-ways. Equally, providing enhanced information on the FMC and live/dead status of trees adjacent to these power line right-of-ways could help land managers decide where to conduct proactive vegetation reduction and removal actions to lower risks associated with dead branches interacting with the power lines and producing burning debris that in turn may ignite the live vegetation on the ground. Recent efforts applying the same UAS data collection and processing workflows have been able to perform all point cloud and tree detection processing steps in 0.5 to 2.0 min ha^{-1} (Tinkham and Woolsey 2024). The use of these analysis strategies is becoming increasingly scalable for management applications.

Limitations

While our UAS-derived model successfully identified the gradient of relative FMC and demonstrated utility for forest management applications, several limitations should be considered when applying these findings. This study was limited to two sites; each representing different management histories and stand structures. Expanding the number of sites and sampled trees could provide insight into the transference of these models across broader forest conditions. Additionally, species was an important predictor of FMC, meaning consideration of the forest tree species will be important in efforts to apply our model. Some studies have successfully classified tree species from UAS multispectral imagery achieving between 55.5% and 81.2% accuracies (Abdollahnegjad and Pangagiotidis 2020; Grybas and Congalton 2021), which may be applied using the same UAS data as those collected for FMC prediction. However, these studies focus on mixed broadleaf and conifer forests, respectively, highlighting a research gap for studies that conduct species classification in mixed-conifer forests. Additionally, the CHM-based tree detection strategy applied in this study is known to have reduced tree detection accuracy of suppressed trees and in areas with canopy cover > 60% (Creasy et al. 2021). However, most trees targeted for retention in these lower montane drought-susceptible forests are overstory individuals. Thus, these methods will likely be employe to target the larger and more fire-resistant trees that these methods were developed to assess.

Temporal variability in FMC presents another challenge. FMC is highly dynamic and can change significantly in response to short-term environmental conditions, such as diurnal fluctuations, seasonal precipitation, and drought stress (Keyes 2006).

At each site, greater FMC and spectral reflectance values were observed during the later collection date. In northern Colorado, late summer (i.e., July–September) precipitation is delivered by the North American monsoon which provides crucial moisture for forests and plays an important role during the end of the fire season (Nauslar et al. 2019). This spectral variation is compounded by changing foliage, with older overwintered needles likely decreasing NIR reflectance in the spring, while new needles will have increased NIR reflectance (Rautianinen et al. 2018). Seasonal changes in needle spectra and within-tree variability in FMC are likely driven by tree biochemical and structural changes (Keyes 2006; Rautiainen et al. 2018). This inverse relationship between needle age and near-infrared (NIR) reflectance may smooth out seasonal dynamics in mature trees with multi-age needles, but our understanding of these spectral and temporal dynamics in semi-arid systems is still underdeveloped. Overall, our data features variability in both observed FMC and spectral reflectance across sites and collection dates that reflect the heterogenous condition of mature forests. These seasonal and within-tree variations may complicate the application of static models for FMC prediction and highlight the importance of testing the relative persistence of how individual trees rank within a site's moisture gradient through time or targeting UAS monitoring of FMC for time periods known to have lower FMC fluctuations (Philpot 1965).

The feasibility of integrating UAS-derived FMC models into operational forest management also depends on logistical considerations, including the scale of data collection, image processing time, accuracy assessments, and computing resources required for model application. Currently, UAS-based efforts are constrained by flight time and regulatory restrictions related to a pilot's line-of-sight to the aircraft, which may impact their effectiveness for characterizing large extents in rugged terrain. Additionally, UAS surveys generate large datasets, requiring significant processing time and technical expertise, which may limit their practical use in large-scale forest assessments or rapid decision making. Despite these limitations, our study demonstrates potential for UAS-derived models to inform targeted management actions, particularly for identifying drought-stressed trees and monitoring treatment effectiveness. However, operationalizing UAS strategies for moisture-stress mapping will need to ensure reliable transference between sites as there are known limitations in the ability of standard train/test split and cross validation approaches during model fitting (Subedi 2023). Particularly in addressing spatial autocorrelation among samples that may inflate estimates of model accuracy (Mayer 2018). Future efforts could benefit from focusing on refining species classification methods, improving FMC models across broader temporal and spatial scales, optimizing data processing workflows, and integrating abiotic predictors (e.g., terrain and weather) to enhance the operational feasibility of UAS-based forest health assessments.

Conclusions

Our analysis identified the most stressed trees at two sites in northern Colorado at 6% precision of foliar moisture content, representing a significant advancement in the tools available for adaptive management in a semi-arid, forested environment.

As aridity is expected to increase in the coming years, UAS monitoring of individual tree drought stress could provide valuable insights to guide targeted treatments aimed at enhancing forest resilience to future disturbances. Managers can integrate these strategies with site-specific knowledge and maps of tree composition and distribution to make fully informed decisions. This would allow managers to prioritize areas for intervention and restoration while accounting for both overstory relative FMC, as well as underlying soil conditions. Foliar moisture content is an important indicator of tree stress and UAS-derived models, as used here, show promising advancements in our understanding and mapping of trees at the forefront of forest change.

Supplementary Information The online version contains supplementary material available at https://doi.org/10.1007/s44391-026-00070-y.

Acknowledgements We would like to thank George Woolsey, Gunnar Ohlson, Kate Johnston, Katarina Warnick, Rylee Askamit, Parker Waterman, and Max Pohl for their assistance with field work and sample processing. Additionally, we would like to thank the Ben Delatour Scout Ranch for access to their land for this study.

Authors' Contributions Conceptualization: Lauren Lad, Wade Tinkham, Camille Stevens-Rumann, Alistair Smith; Methodology: Lauren Lad, Wade Tinkham, Camille Stevens-Rumann; Formal analysis and investigation: Lauren Lad and Wade Tinkham; Writing – original draft preparation: Lauren Lad; Writing – review and editing: Lauren Lad, Wade Tinkham, Camille Stevens-Rumann, Jody Vogeler, Melanie Vanderhoof, Alistair Smith; Funding acquisition: Lauren Lad, Wade Tinkham, Camille Stevens-Rumann, Alistair Smith.

Funding This work is funded under the USDA Hatch (COL00401), Joint Fire Science Program Graduate Research Innovation (23–1-01–24) programs, and Colorado Forest Restoration Institute Appropriations funding. With additional support from the US Department of Agriculture's National Institute of Food and Agriculture program (2022–67021-37857) and U.S. Department of Agriculture, Forest Service with funding from the Infrastructure Investment and Jobs Act (24-JV-11221633–195). This research was supported by the U.S. Department of Agriculture, Forest Service, Rocky Mountain Research Station. The findings and conclusions in this publication are those of the authors and should not be construed to represent any official USDA or US Government determination or policy. The findings and conclusions in this publication are those of the authors and should not be construed to represent any official USDA determination or policy. Any use of trade, firm, or product names is for descriptive purposes only and does not imply endorsement by the U.S. Government.

Data Availability Data will be made available on reasonable request.

Declarations

Conflict of interest The authors declare that they have no conflict of interest.

References

Abdollahnejad, A., and D. Panagiotidis. 2020. Tree species classification and health status assessment for a mixed broadleaf-conifer forest with UAS multispectral imaging. *Remote Sensing* 12 (22): Article 22. https://doi.org/10.3390/rs12223722.

Allen, C.D., A.K. Macalady, H. Chenchouni, D. Bachelet, N. McDowell, M. Vennetier, T. Kitzberger, A. Rigling, D.D. Breshears, E.H.(T.) Hogg, P. Gonzalez, R. Fensham, Z. Zhang, J. Castro, N. Demidova, J.-H. Lim, G. Allard, S.W. Running, A. Semerci, and N. Cobb. 2010. A global overview of drought and heat-induced tree mortality reveals emerging climate change risks for forests. *Forest Ecology and Management* 259 (4): 660–684. https://doi.org/10.1016/j.foreco.2009.09.001.

Anderegg, W. R. L., A. G. Konings, A. T. Trugman, K. Yu, D. R. Bowling, R. Gabbitas, D. S. Karp, S. Pacala, J. S. Sperry, B. N. Sulman, and N. Zenes. 2018. Hydraulic diversity of forests regulates ecosystem resilience during drought. *Nature* 561 (7724): 538–541. https://doi.org/10.1038/s41586-018-0539-.

Anderegg, W.R.L., L.D.L. Anderegg, and C. Huang. 2019a. Testing early warning metrics for drought-induced tree physiological stress and mortality. *Global Change Biology* 25 (7): 2459–2469. https://doi.org/10.1111/gcb.14655.

Anderegg, W.R.L., L.D.L. Anderegg, K.L. Kerr, and A.T. Trugman. 2019b. Widespread drought-induced tree mortality at dry range edges indicates that climate stress exceeds species' compensating mechanisms. *Global Change Biology* 25 (11): 3793–3802. https://doi.org/10.1111/gcb.14771.

Andrews, C. M., A. W. D'Amato, S. Fraver, B. Palik, M. A. Battaglia, and J. B. Bradford. 2020. Low stand density moderates growth declines during hot droughts in semi-arid forests. *Journal of Applied Ecology* 57 (6): 1089–1102. https://doi.org/10.1111/1365-2664.13615

Baston, D. 2020. exactextractr: fast extraction from raster datasets using polygons. R package version 0.10.0. https://github.com/isciences/exactextractr

Batllori, E., F. Lloret, T. Aakala, W.R.L. Anderegg, E. Aynekulu, D.P. Bendixsen, A. Bentouati, C. Bigler, C.J. Burk, J.J. Camarero, M. Colangelo, J.D. Coop, R. Fensham, M.L. Floyd, L. Galiano, J.L. Ganey, P. Gonzalez, A.L. Jacobsen, J.M. Kane, Thomas Kitzberger, Juan C... Linares, Suzanne B... Marchetti, George Matusick, Michael Michaelian, Rafael M... Navarro-Cerrillo, Robert Brandon Pratt, Miranda D... Redmond, Andreas Rigling, Francesco Ripullone, Gabriel Sangüesa-Barreda, Yamila Sasal, Sandra Saura-Mas, Maria Laura Suarez, Thomas T... Veblen, Albert Vilà-Cabrera, Caroline Vincke, and B. Zeeman. 2020. Forest and woodland replacement patterns following drought-related mortality. *Proceedings of the National Academy of Sciences* 117 (47): 29720–29729. https://doi.org/10.1073/pnas.2002314117.

Blanco, V., P.J. Blaya-Ros, C. Castillo, F. Soto-Vallés, R. Torres-Sánchez, and R. Domingo. 2020. Potential of UAS-based remote sensing for estimating tree water status and yield in sweet cherry trees. *Remote Sensing* 12 (15): Article 15. https://doi.org/10.3390/rs12152359.

Bolinger, R., J. Lukas, R. Schumacher, and P. Goble. 2023. *Climate change in Colorado*. https://hdl.handle.net/10217/237323

Bond, W. J., and J. E. Keeley. 2005. Fire as a global 'herbivore': the ecology and evolution of flammable ecosystems. *Trends in ecology & evolution* 20 (7): 387–394. https://doi.org/10.1016/j.tree.2005.04.025

Breiman, L. 2001. Random forests. *Machine Learning* 45 (1): 5–32 10.1023/A:1010933404324.

Breshears, D.D., N.S. Cobb, P.M. Rich, K.P. Price, C.D. Allen, R.G. Balice, W.H. Romme, J.H. Kastens, M.L. Floyd, J. Belnap, J.J. Anderson, O.B. Myers, and C.W. Meyer. 2005. Regional vegetation die-off in response to global-change-type drought. *Proceedings of the National Academy of Sciences* 102 (42): 15144–15148. https://doi.org/10.1073/pnas.0505734102.

Brown, T.P., Z.H. Hoylman, E. Conrad, Z. Holden, K. Jencso, and W.M. Jolly. 2022. Decoupling between soil moisture and biomass drives seasonal variations in live fuel moisture across co-occurring plant functional types. *Fire Ecology* 18 (1): 14. https://doi.org/10.1186/s42408-022-00136-5.

Canty, A., and B. D. Ripley. 2022. boot: Bootstrap R (S-Plus) Functions (R package version 1.3-28.1). https://cran.r-project.org/web/packages/boot/boot.pdf

Churchill, D. J., A. J. Larson, M. C. Dahlgreen, J. F. Franklin, P. F. Hessburg, and J. A. Lutz. 2013. Restoring forest resilience: from reference spatial patterns to silvicultural prescriptions and monitoring. *Forest Ecology and Management* 291:442–457. https://doi.org/10.1016/j.foreco.2012.11.007

Cook, B.I., T.R. Ault, and J.E. Smerdon. 2015. Unprecedented 21st century drought risk in the American Southwest and Central Plains. *Science Advances* 1 (1): e1400082. https://doi.org/10.1126/sciadv.1400082.

Cook, B.I., J.S. Mankin, and K.J. Anchukaitis. 2018. Climate change and drought: From past to future. *Current Climate Change Reports* 4 (2): 164–179. https://doi.org/10.1007/s40641-018-0093-2.

Coop, J.D., S.A. Parks, C.S. Stevens-Rumann, S.D. Crausbay, P.E. Higuera, M.D. Hurteau, A. Tepley, E. Whitman, T. Assal, B.M. Collins, K.T. Davis, S. Dobrowski, D.A. Falk, P.J. Fornwalt, P.Z. Fulé, B.J. Harvey, V.R. Kane, C.E. Littlefield, E.Q. Margolis, M. North, M.A. Parisien, S. Prichard, and K.C. Rodman. 2020. Wildfire-driven forest conversion in western North American landscapes. *BioScience* 70 (8): 659–673. https://doi.org/10.1093/biosci/biaa061.

Creasy, M.B., W.T. Tinkham, C.M. Hoffman, and J.C. Vogeler. 2021. Potential for individual tree monitoring in ponderosa pine-dominated forests using unmanned aerial system structure from motion point clouds. *Canadian Journal of Forest Research* 51: 1093–1105. https://doi.org/10.1139/cjfr-2020-0433.

Cruz, M. G., and M. E. Alexander. 2013. Uncertainty associated with model predictions of surface and crown fire rates of spread. *Environmental Modelling & Software* 47:16–28. https://doi.org/10.1016/j.envsoft.2013.04.004

Davison, A. C., and D. V. Hinkley. 1997. *Bootstrap methods and their application*. Cambridge University Press

D'Odorico, P., L. Schönbeck, V. Vitali, K. Meusburger, M. Schaub, C. Ginzler, R. Zweifel, V.M.E. Velasco, J. Gisler, A. Gessler, and I. Ensminger. 2021. Drone-based physiological index reveals long-term acclimation and drought stress responses in trees. *Plant, Cell & Environment* 44 (11): 3552–3570. https://doi.org/10.1111/pce.14177.

Davis, K.T., J. Peeler, J. Fargione, R.D. Haugo, K.L. Metlen, M.D. Robles, and T. Woolley. 2024. Tamm review: A meta-analysis of thinning, prescribed fire, and wildfire effects on subsequent wildfire severity in conifer dominated forests of the Western US. *Forest Ecology and Management* 561: 121885. https://doi.org/10.1016/j.foreco.2024.121885.

Ewane, E. B., M. Mohan, S. Bajaj, G. P. Galgamuwa, M. S. Watt, P. P. Arachchige, and A. Cardil. 2023. Climate-change-driven droughts and tree mortality: assessing the potential of UAV-derived early warning metrics. *Remote Sensing* 15 (10): 2627. https://doi.org/10.3390/rs15102627

Ezenne, G.I., L. Jupp, S.K. Mantel, and J.L. Tanner. 2019. Current and potential capabilities of UAS for crop water productivity in precision agriculture. *Agricultural Water Management* 218: 158–164. https://doi.org/10.1016/j.agwat.2019.03.034.

Faiella, S.M., and J.D. Bailey. 2007. Fluctuations in fuel moisture across restoration treatments in semi-arid ponderosa pine forests of Norther Arizona, USA. *International Journal of Wildland Fire* 16 (1): 119–127. https://doi.org/10.1071/WF06018.

Finley, K., and J. Zhang. 2019. Climate effect on ponderosa pine radial growth varies with tree density and shrub removal. *Forests* 10 (6): 477. https://doi.org/10.3390/f10060477

Flannigan, M.D., B.M. Wotton, G.A. Marshall, W.J. de Groot, J. Johnston, N. Jurko, and A.S. Cantin. 2016. Fuel moisture sensitivity to temperature and precipitation: Climate change implications. *Climatic Change* 134 (1): 59–71. https://doi.org/10.1007/s10584-015-1521-0.

Fraser, B.T., and R.G. Congalton. 2021. Monitoring fine-scale forest health using unmanned aerial systems (UAS) multispectral models. *Remote Sensing* 13 (23): 23. https://doi.org/10.3390/rs13234873.

Gao, B. 1996. NDWI—A normalized difference water index for remote sensing of vegetation liquid water from space. *Remote Sensing of Environment* 58 (3): 257–266. https://doi.org/10.1016/S0034-4257(96)00067-3.

Garza, B.N., V. Ancona, J. Enciso, H.L. Perotto-Baldivieso, M. Kunta, and C. Simpson. 2020. Quantifying citrus tree health using true color UAV images. *Remote Sensing* 12 (1): Article 1. https://doi.org/10.3390/rs12010170.

Groover, A. (2017). Age-Related Changes in Tree Growth and Physiology. In John Wiley & Sons, Ltd (Ed.), *eLS* (1st ed., pp. 1–7). Wiley. https://doi.org/10.1002/9780470015902.a0023924

Grulke, N., J. Maxfield, P. Riggan, and C. Schrader-Patton. 2020. Pre-emptive detection of mature pine drought stress using multispectral aerial imagery. *Remote Sensing* 12 (14): Article 14. https://doi.org/10.3390/rs12142338.

Grybas, H., and R. G. Congalton. 2021. A comparison of multi-temporal RGB and multispectral UAS imagery for tree species classification in heterogeneous New Hampshire Forests. *Remote Sensing* 13 (13): 2631. https://doi.org/10.3390/rs13132631

Hanna, L., W.T. Tinkham, M.A. Battaglia, J.C. Vogeler, S.M. Ritter, and C.M. Hoffman. 2024. Characterizing heterogeneous forest structure in Ponderosa pine forests via UAS-derived structure from motion. *Environmental Monitoring and Assessment* 196 (6): 530. https://doi.org/10.1007/s10661-024-12703-1.

Hebbali, A. 2020. Olsrr: Tools for building OLS regression models (Version 0.5.3). CRAN. https://CRAN.R-project.org/package=olsrr

Hogland, J. S. 2019. Estimates of Forest Characteristics Derived from Remotely Sensed Imagery and Field Samples: Applicable Scales, Appropriate Study Design, and Relevance to Forest Management. University of Montana.

Humagain, K., C. Portillo-Quintero, R. D. Cox, and J. W. Cain III. 2017. Mapping tree density in forests of the southwestern USA using Landsat 8 data. *Forests* 8 (8): 287. https://doi.org/10.3390/f8080287

Jemaa, H., W. Bouachir, B. Leblon, A. LaRocque, A. Haddadi, and N. Bouguila. 2023. UAV-based computer vision system for orchard apple tree detection and health assessment. *Remote Sensing* 15 (14): Article 14. https://doi.org/10.3390/rs15143558.

Jolly, W.M., and A.M. Hadlow. 2012. A comparison of two methods for estimating conifer live foliar moisture content. *International Journal of Wildland Fire* 21 (2): 180. https://doi.org/10.1071/WF11015.

Jolly, W. M., and D. M. Johnson. 2018. Pyro-ecophysiology: Shifting the paradigm of live wildland fuel research. *Fire* 1 (1) : 8 (**10.3390/fire1010008**).

Joseph, J., J. Luster, A. Bottero, N. Buser, L. Baechli, K. Sever, and A. Gessler. 2021. Effects of drought on nitrogen uptake and carbon dynamics in trees. *Tree Physiology* 41 (6): 927–943. https://doi.org/10.1093/treephys/tpaa146.

Keyes, Christopher R. 2006. Foliar Moisture Contents of North American Conifers. In: Andrews, Patricia L.; Butler, Bret W., comps. 2006. Fuels Management-How to Measure Success: Conference Proceedings. 28–30 March 2006; Portland, OR. Proceedings RMRS-P-41. Fort Collins, CO: U.S. Department of Agriculture, Forest Service, Rocky Mountain Research Station. p. 395–399

Kreuzwieser, J., and A. Gessler. 2010. Global climate change and tree nutrition: Influence of water availability. *Tree Physiology* 30 (9): 1221–1234. https://doi.org/10.1093/treephys/tpq055.

Lad, L.E., W.T. Tinkham, A.M. Sparks, and A.M.S. Smith. 2023. Evaluating predictive models of tree foliar moisture content for application to multispectral UAS data: A laboratory study. *Remote Sensing* 15 (24): Article 24. https://doi.org/10.3390/rs15245703.

Larcher, W. (2003). Physiological Plant Ecology: Ecophysiology and Stress Physiology of Functional Groups. Springer. Berlin, Germany. p 514. ISBN: 978–3–540–43516–7.

Larson, A. J., and D. Churchill. 2012. Tree spatial patterns in fire-frequent forests of Western North America, including mechanisms of pattern formation and implications for designing fuel reduction and restoration treatments. *Forest Ecology & Management* 267:74–92. https://doi.org/10.1016/j.foreco.2011.11.038.

Lentile, L.B., Z.A. Holden, A.M.S. Smith, M.J. Falkowski, A.T. Hudak, P. Morgan, S.A. Lewis, P.E. Gessler, and N.C. Benson. 2006. Remote sensing techniques to assess active fire characteristics and post-fire effects. *International Journal of Wildland Fire* 15 (3): 319. https://doi.org/10.1071/WF05097.

Liaw, A., and M. Wiener. 2002. Classification and regression by randomForest. *R News* 2 (3): 18–22.

Littell, J.S., D.L. Peterson, K.L. Riley, Y. Liu, and C.H. Luce. 2016. A review of the relationships between drought and forest fire in the United States. *Global Change Biology* 22 (7): 2353–2369. https://doi.org/10.1111/gcb.13275.

Liu, J., L. Gao, F. Yuan, Y. Guo, and X. Xu. 2019. Climate change made major contributions to soil water storage decline in the Southwestern US during 2003–2014. *Water* 11 (9): Article 9. https://doi.org/10.3390/w11091947.

Marques, P., L. Pádua, J. Sousa, and A. Fernandes-Silva. 2023. Assessing the water status and leaf pigment content of olive trees: Evaluating the potential and feasibility of unmanned aerial vehicle multispectral and thermal data for estimation purposes. *Remote Sensing* 15 : 4777. https://doi.org/10.3390/rs15194777.

Mast, J. N., T. T. Veblen, and Y. B. Linhart. 1998. Disturbance and climatic influences on age structure of ponderosa pine at the pine/grassland ecotone, Colorado Front Range. *Journal of Biogeography* 25 (4): 743–755. https://doi.org/10.1046/j.1365-2699.1998.2540743.x.

Matthews, S. 2010. Effect of drying temperature on fuel moisture content measurements. *International Journal of Wildland Fire* 19 (6): 800. https://doi.org/10.1071/wf08188.

Matus, P., R. Nasi, E. Honkavaara, M. Blazenec, J. Skvarenina, R. Modlinger, J. Roznovsky, and R. Jakus. 2025. Spectral signatures discrimination of Norway spruce trees under experimentally induced drought and acute thermal stress using hyperspectral imaging. *Forest Ecology and Management* 586 : 122692. https://doi.org/10.1016/j.foreco.2025.122692.

Meyer, H., C. Reudenbach, T. Hengl, M. Katurji, and T. Nauss. 2018. Improving performance of spatio-temporal machine learning models using forward feature selection and target oriented validation. *Environmental Modelling and Software* 101: 1–9. https://doi.org/10.1016/j.envsoft.2017.12.001.

Näsi, R., E. Honkavaara, M. Blomqvist, P. Lyytikäinen-Saarenmaa, T. Hakala, N. Viljanen, and M. Holopainen. 2018. Remote sensing of bark beetle damage in urban forests at individual tree level using a novel hyperspectralcamera from UAV and aircraft. *Urban Forestry & Urban Greening* 30:72–83. https://doi.org/10.1016/j.ufug.2018.01.010

Nauslar, N.J., B.J. Hatchett, T.J. Brown, M.L. Kaplan, and J.F. Mejia. 2019. Impact of the North American Monsoon on wildfire activity in the Southwest United States. *International Journal of Climatology* 39 (3): 1539–1554. https://doi.org/10.1002/joc.5899.

North, M., M. Hurteau, and J. Innes. 2009. Fire suppression and fuels treatment effects on mixed-conifer carbon stocks and emissions. *Ecological applications* 19 (6): 1385–1396. https://doi.org/10.1890/08-1173.1

Pádua, L., P. Marques, L. Martins, A. Sousa, E. Peres, and J.J. Sousa. 2020. Monitoring of chestnut trees using machine learning techniques applied to UAV-based multispectral data. *Remote Sensing* 12 (18): Article 18. https://doi.org/10.3390/rs12183032.

Park Williams, A., C.D. Allen, A.K. Macalady, D. Griffin, C.A. Woodhouse, D.M. Meko, T.W. Swetnam, S.A. Rauscher, R. Seager, H.D. Grissino-Mayer, J.S. Dean, E.R. Cook, C. Gangodagamage, M. Cai, and N.G. McDowell. 2013. Temperature as a potent driver of regional forest drought stress and tree mortality. *Nature Climate Change* 3 (3): 292–297. https://doi.org/10.1038/nclimate1693.

Pebesma, E. 2018. Simple features for R: Standardized support for spatial vector data. *The R Journal* 10 (1): 439–446. https://doi.org/10.32614/RJ-2018-009.

Pérez-Rodríguez, L.A., C. Quintano, E. Marcos, S. Suarez-Seoane, L. Calvo, and A. Fernández-Manso. 2020. Evaluation of prescribed fires from unmanned aerial vehicles (UAVs) imagery and machine learning algorithms. *Remote Sensing* 12 (8): 1295. https://doi.org/10.3390/rs12081295.

Philpot, C. W. 1965. Diurnal fluctuation in moisture content of ponderosa pine and white leaf manzanita leaves. U.S. Department of Agriculture, Forest Service Research Note PSW-RN-67. 7 p.

Phiri, D., M. Simwanda, S. Salekin, V. R. Nyirenda, Y. Murayama, and M. Ranagalage. 2020. Sentinel-2 data for land cover/use mapping: A review. *Remote sensing* 12 (14): 2291. https://doi.org/10.3390/rs12142291

Pierce, L.L., S.W. Running, and G.A. Riggs. 1990. Remote detection of canopy water stress in coniferous forests using the NS001 Thematic Mapper Simulator and the Thermal Infrared Multispectral Scanner. *Photogrammetric Engineering and Remote Sensing* 56 (5): 579–586.

Prichard, S. J., N. A. Povak, M. C. Kennedy, and D. W. Peterson. 2020. Fuel treatment effectiveness in the context of landform, vegetation, and large, wind-driven wildfires. *Ecological Applications* 30 (5) : e02104. https://doi.org/10.1002/eap.2104.

Rautiainen, M., P. Lukeš, L. Homolová, A. Hovi, J. Pisek, and M. Mõttus. 2018. Spectral properties of coniferous forests: A review of in situ and laboratory measurements. *Remote Sensing* 10 (2): 207. https://doi.org/10.3390/rs10020207

R Core Team. 2023. *R: A Language and Environment for Statistical Computing*. Vienna, Austria: R Foundation for Statistical Computing.

Rock, B. N., D. L. Williams, D. M. Moss, G. N. Lauten, and M. Kim. 1994. High-spectral resolution field and laboratory optical reflectance measurements of red spruce and eastern hemlock needles and branches. *Remote Sensing of Environment* 47 (2): 176–189. https://doi.org/10.1016/0034-4257(94)90154-6.

Rouse, J. W., Haas, R. H., Schell, J. A., & Deering, D. W. (1974). *Monitoring vegetation systems in the Great Plains with ERTS*. https://ntrs.nasa.gov/citations/19740022614

Roussel, J.R., D. Auty, N.C. Coops, P. Tompalski, T.R.H. Goodbody, A. Sánchez Meador, J.F. Bourdon, F. De Boissieu, and A. Achim. 2020. lidR : An R package for analysis of airborne laser scanning (ALS) data. *Remote Sensing of Environment* 251: 112061. https://doi.org/10.1016/j.rse.2020.112061.

Roussel, J. R., Auty, D. (2024). Airborne LiDAR Data Manipulation and Visualization for Forestry Applications. R package version 4.1.0. https://cran.r-project.org/package=lidR

Roussel J (2024). _lasR: Fast and Pipeable Airborne LiDAR Data Tools_. R package version 0.5.6, https://github.com/r-lidar/lasR

Ruthrof, K. X., J. B. Fontaine, G. Matusick, D. D. Breshears, D. J. Law, S. Powell, and G. Hardy. 2016. How drought-induced forest die-off alters microclimate and increases fuel loadings and fire potentials. *International Journal of Wildland Fire* 25 (8): 819–830. https://doi.org/10.1071/WF15028.

Ryan, M. G. 2011. Tree responses to drought. *Tree Physiology* 31 (3): 237–239. https://doi.org/10.1093/treephys/tpr022.

Ryan, K.C., E.E. Knapp, and J.M. Varner. 2013. Prescribed fire in North American forests and woodlands: History, current practice, and challenges. *Frontiers in Ecology and the Environment* 11 (s1): e15–e24. https://doi.org/10.1890/120329.

Simonin, K., T. E. Kolb, M. Montes-Helu, and G. W. Koch. 2007. The influence of thinning on components of stand water balance in a ponderosa pine forest stand during and after extreme drought. *Agricultural and Forest Meteorology* 143 (3-4): 266–276. https://doi.org/10.1016/j.agrformet.2007.01.003

Schwilk, D.W., M.A. Alam, N. Gill, B.R. Murray, R.H. Nolan, S. Ondei, G.L.W. Perry, A.M.S. Smith, D.M.J.S. Bowman, A. Fidelis, P. Jaureguiberry, I.O. Menor, B.H.P. Rosado, H. Roland, M. Yebra, S.G. Yelenik, and T.J. Curran. 2025. From plant traits to fire behavior: Scaling issues in flammability studies. *American Journal of Botany*. https://doi.org/10.1002/ajb2.70040.

Sparks, A., C. Kolden, A. Talhelm, A. Smith, K. Apostol, D. Johnson, and L. Boschetti. 2016. Spectral indices accurately quantify changes in seedling physiology following fire: Towards mechanistic assessments of post-fire carbon cycling. *Remote Sensing* 8 (7): 572. https://doi.org/10.3390/rs8070572.

Sparks, A. M., A. S. Blanco, L. E. Lad, A. M. Smith, H. D. Adams, and W. T. Tinkham. 2024. Prefire drought intensity drives postfire recovery and mortality in Pinus monticola and Pseudotsuga menziesii saplings. *Forest Science* 70 (3), 189–201. https://doi.org/10.1093/forsci/fxae013

Stephens, S.L., B.M. Collins, C.J. Fettig, M.A. Finney, C.M. Hoffman, E.E. Knapp, M.P. North, H. Safford, and R.B. Wayman. 2018. Drought, tree mortality, and wildfire in forests adapted to frequent fire. *BioScience* 68 (2): 77–88. https://doi.org/10.1093/biosci/bix146.

Subedi, M. R., C. Portillo-Quintero, S. S. Kahl, N. E. McIntyre, R. D. Cox, and G. Perry. 2023. Leveraging NAIP imagery for accurate large-area land use/land cover mapping: A case study in Central Texas. *Photogrammetric Engineering & Remote Sensing* 89 (9): 547–560. https://doi.org/10.3390/rs16152778.

Swayze, N.C., W.T. Tinkham, J.C. Vogeler, and A.T. Hudak. 2021. Influence of flight parameters on UAS-based monitoring of tree height, diameter, and density. *Remote Sensing of Environment* 263: 112540. https://doi.org/10.1016/j.rse.2021.112540.

Tinkham, W.T., and N.C. Swayze. 2021. Influence of Agisoft Metashape parameters on UAS structure from motion individual tree detection from canopy height models. *Forests* 12 (2): Article 2. https://doi.org/10.3390/f12020250.

Tinkham, W.T., and G.A. Woolsey. 2024. Influence of structure from motion algorithm parameters on metrics for individual tree detection accuracy and precision. *Remote Sensing* 16 (20): 3844. https://doi.org/10.3390/rs16203844.

Tinkham, W.T., N.C. Swayze, C.M. Hoffman, L.E. Lad, and M.A. Battaglia. 2022. Modeling the missing DBHs: Influence of model form on UAV DBH characterization. *Forests* 13 (12): Article 12. https://doi.org/10.3390/f13122077.

Vicca, S., M. Balzarolo, I. Filella, A. Granier, M. Herbst, A. Knohl, and J. Peñuelas. 2016. Remotely-sensed detection of effects of extreme droughts on gross primary production. *Scientific Reports* 6 (1): 28269. https://doi.org/10.1038/srep28269

Williams, J. W. 2022. RAD: A paradigm, shifting. *BioScience* 72 (1): 13–15. https://doi.org/10.1093/biosci/biab123.

Williams, A. P., E. R. Cook, J. E. Smerdon, B. I. Cook, J. T. Abatzoglou, K. Bolles, S. H. Baek, A. M. Badger, and B. Livneh. 2020. Large contribution from anthropogenic warming to an emerging North American megadrought. *Science* 368 (6488): 314–318. https://doi.org/10.1126/science.aaz9600.

Woolsey. G., & Tinkham, W.T. (2024). _cloud2trees: Point Cloud Data to Forest Inventory Tree List_. R package version 0.2.0. https://github.com/georgewoolsey/cloud2trees

Young, D. J., B. L. Estes, S. Gross, A. Wuenschel, C. Restaino, and M. D. Meyer. 2023. Effectiveness of forest density reduction treatments for increasing drought resistance of ponderosa pine growth. *Ecological Applications* 33 (4): e2854. https://doi.org/10.1002/eap.2854

Zarco-Tejada, P. J., A. Catalina, M. R. González, and P. Martín. 2013. Relationships between net photosynthesis and steady-state chlorophyll fluorescence retrieved from airborne hyperspectral imagery. *Remote Sensing of Environment* 136:247–258. https://doi.org/10.1016/j.rse.2013.05.011

Zhang, J., J. Hu, J. Lian, Z. Fan, X. Ouyang, and W. Ye. 2016. Seeing the forest from drones: Testing the potential of lightweight drones as a tool for long-term forest monitoring. *Biological Conservation* 198:60–69. https://doi.org/10.1016/j.biocon.2016.03.027.

Zhang, J., K. A. Finley, N. G. Johnson, and M. W. Ritchie. 2019. Lowering stand density enhances resiliency of Ponderosa Pine forests to disturbances and climate change. *Forest Science* 65 (4): 496–507. https://doi.org/10.1093/forsci/fxz006.

Zhou, J.-J., Y.-H. Zhang, Z.-M. Han, X.-Y. Liu, Y.-F. Jian, C.-G. Hu, and Y.-Y. Dian. 2021. Evaluating the performance of hyperspectral leaf reflectance to detect water stress and estimation of photosynthetic capacities. *Remote Sensing* 13 (11) : 2160. https://doi.org/10.3390/rs13112160.

Authors and Affiliations

Lauren E. Lad[1] · Wade T. Tinkham[2] · Camille S. Stevens-Rumann[1] · Melanie Vanderhoof[3] · Jody Vogeler[4] · Alistair M. S. Smith[5]

✉ Lauren E. Lad
lauren.lad@colostate.edu

Wade T. Tinkham
wade.tinkham@usda.gov

Camille S. Stevens-Rumann
c.stevens-rumann@colostate.edu

Melanie Vanderhoof
mvanderhoof@usgs.gov

Jody Vogeler
jody.vogeler@colostate.edu

Alistair M. S. Smith
alistair@uidaho.edu

1 Department of Forest and Rangeland Stewardship, Colorado State University, 1001 Amy Van Dyken Way, Fort Collins CO 80523, USA

2 U.S. Department of Agriculture, Forest Service, Rocky Mountain Research Station, 240 W Prospect Road, Fort Collins CO 80526, USA

3 Geosciences and Environmental Change Science Center, US Geological Survey, Denver Federal Center, MS980, Denver CO 80225, USA

4 Natural Resources Ecology Laboratory, Colorado State University, Fort Collins CO 80523, USA

5 Department of Earth and Spatial Sciences, College of Science, University of Idaho, Moscow ID 83844, USA